Bayesian reconstruction of the Milky Way dark matter distribution

Caterina Prior & Keerthana Umesh

January 17, 2025

Abstract

In this study, we employed a Bayesian workflow to find the dark matter distribution in the Milky Way galaxy and estimate the local dark matter density. In particular, we aimed to provide some clarification into the underlying causes of dips in the rotation curve typically observed within the 10 - 20 kpc range. We fit computationally simple, axisymmetric models to existing kinematic data (rotation curves) of visible matter in the Milky Way extending to $\sim$ 100kpc from the galactic center. The results demonstrate that a dark matter model which incorporates a Navarro-Frenk-White profile and two ring-like overdensities in the region of the dips leads to a more robust fit, as suggested by the χ^2, DIC and Bayes-ratio values. This suggests that the rotation curve dips are best explained as phenomenological features of the dark matter distribution. The model results in a corresponding local dark matter density of $\rho_0 = 1.170 \pm 0.031\ GeV\ cm^{-3}$, three times larger than simpler models that do not account for the dips. This has a significant impact on the expected dark matter interaction rates for Earth-based detectors.

1 Introduction

The nature of dark matter remains a key question in modern cosmology. One effective method to study the dark matter distribution in a galaxy uses its rotation curve, which plots the circular velocities of its stellar components at different radii from the galactic center. In most galaxies, the extent of the visible matter component should result in a Keplerian decline at large radii, but the rotation curve is often observed to plateau, indicating the presence of an unseen "halo" of mass, i.e. dark matter [1]. We can infer the galaxy's dark matter distribution by fitting the observed rotation curve to velocities predicted from the visible (mostly stellar) matter distribution, and match the difference to different hypothesized dark matter distributions [2].

In this study, we employ a Bayesian probabilistic workflow to determine the dark matter distribution of the Milky Way, to the end of estimating the *local dark matter density*, i.e. the density in the solar neighborhood. This is an important metric for Earth-based dark matter searches as it informs the expected interaction rate, which is used to calibrate detectors and benchmark different particle physics models [3]. The significant systematic biases and uncertainties associated with empirical astronomical constants, stellar motion observations, and distance measurements limit the reliability of point estimates. A Bayesian treatment is better suited for such analyses, and it also has a framework to incorporate prior information from previous studies of the Milky Way's dark matter distribution.

We use the velocity curve of the Milky Way reported by Huang et. al [4]. This is one of the most comprehensive reconstructions with measurements extending to large radii ($\sim$100 kpc) where dark matter dominates. The study uses spectral information and line-of-sight velocity measurements of three stellar populations from the LSS-GAC, (SDSS)-III/APOGEE and SDSS/SEGUE surveys and derives their distances from the galactic center and radial velocities. The results are then binned and the final rotation velocities are reported at the radius of the center of each bin with the weighted average and standard deviation of the velocities. Each bin has at least 80 tracer measurements which are Gaussian distributed around the average velocity [4].

A key feature of this dataset is the presence of dips in the rotation curve at 11kpc and 19kpc from the galactic center (see Appendix B). There are two potential reasons for these dips: (a) they could be artificially caused as a result of measurement uncertainties, or, (b) they may arise from the underlying dark matter distribution. In case of the former, we repeat our basic analysis with datapoints between 10-20 kpc removed to test the robustness of our local dark matter determination. The dips have also been proposed to arise from ring-like structures of dark matter formed by the early infall of a dwarf galaxy [5]. We therefore compare two models in this study, with and without the additional perturbation from the dark matter rings, to test their effect on the local dark matter density.

2 Building the model

To accurately determine the dark matter distribution of the Milky Way, we must first consider what rotation curve we would expect to see from the luminous components. Spiral galaxies can typically be decomposed into a bulge, stellar disk, and dark matter halo component. The mass density of the visible components can be modelled using observationally derived functions,

from which the corresponding velocity curve at each radial position can be found. Various functional forms are available in the literature, with the bulge showing the most variation. We followed the modelling approach from [6] for computational efficiency, which uses simple, axisymmetric models that are still empirically consistent.

Numerous bulge density profiles, including elliptical models, have been proposed for the Milky Way. They are difficult to confirm experimentally due to the high density of stars at our galaxy's center. However, the scale lengths of the bulge are generally accepted to be < 1 kpc. This is smaller than the smallest radius in the chosen dataset ($\sim$ 5kpc), thus we can adopt a spherically symmetric approximation of its shape. We modelled the bulge to consist of an inner and outer component, each one being an exponential sphere. We fixed their scale lengths based on [6] as a=3.5pc and b= 120pc but treated their total mass as a free parameter, allowing the overall normalization to remain unconstrained. This way, the central black hole of the galaxy is also taken into account as a point mass. The circular velocity induced by the bulge potential [6] is:

$$v_{bulge}^2 = G\left[\frac{M_{b,\text{inner}}}{r}F\left(\frac{r}{0.0035}\right) + \frac{M_{b,\text{outer}}}{r}F\left(\frac{r}{0.12}\right)\right] \tag{1}$$

where,

$$F(x) = 1 - e^{-x}(1 + x + x^2/2) \tag{2}$$

Similarly, the Milky Way's stellar disk was modelled as an exponential razor-thin disk with a fixed scale length (< 5 kpc, smaller than our data range), while its total mass was left as a free parameter. This gives a circular velocity:

$$v_{disk}^2 = \frac{2GM_{disk}}{R_d}y^2[I_0(y)K_0(y) - I_1(y)K_1(y)] \tag{3}$$

where $y = \frac{r}{2}r_d$ with the scale radius r_d=4.9kpc. I and K are the modified Bessel functions [7][6]. We treated the total mass normalizations as nuisance parameters, only allowing them to remain free due to the significant variability in their reported values across different models in literature.

Many dark matter distributions have been theorized for spiral galaxies. Here, we adopted the most popular model, namely the spherical Navarro-Frenk-White (NFW) profile whose shape is dependent on two parameters: the scale radius (r_s) and the *local* dark matter density (ρ_0), both of which we leave free: [8]

$$v_{dark\ matter}^2 = \frac{4\pi G\rho_0 G R_0(r_s + R_0)^2}{r}\left[\ln(r_s + r) - \ln(r_s) + \frac{r_s}{r_s + r} - 1\right] \tag{4}$$

Using these three components, we can fit a global model of the galaxy to the observed rotation curve, using

$$v^2(r_s, \rho_0, M_{b,inner}, M_{b,outer}, M_{disk}) = v_{bulge}^2(M_{b,inner}, M_{b,outer}) + v_{disk}^2(M_{disk}) + v_{halo}^2(r_s, \rho_0) \tag{5}$$

where r_s is the scale radius of the dark matter profile, ρ_0 is the dark matter density at the Sun's location, $M_{b,inner}$ and $M_{b,outer}$ represent the masses of the inner and outer bulge respectively, and M_{disk} is the total mass of the stellar disk. These formulae assume the Sun is at a galactocentric radius of $R_0 = 8.34\ kpc$ with a rotational velocity of $v_0 = 239.89\ km/s$, corresponding with [4]. Each term is dependent on r, the radial distance from the galactic center.

As outlined in Section 1, we can assess the robustness of our dark matter determination by refitting the model to a dataset that excludes data points between 10 and 20 kpc, thereby removing the observed dips at 11 and 19 kpc. Alternatively, we also aim to investigate if these dips have a phenomenological cause. Building on previous hypotheses of doughnut-like overdensities of dark matter from [5], our second model incorporated an additional contribution to the dark matter profile from two circular ring-like structures. These ring potentials were incorporated using the `galpy` Python package. To avoid infinite velocities at their centers, we applied Gaussian smoothing, and fixed all parameters to values as reported by [5]. Thus both models share identical parameters, with the second model incorporating an additional contribution from the ring structures.

Literature values for the parameters, particularly the masses, are often poorly constrained due to systematic biases and model dependence. To account for this, we used wide, "uninformative" uniform priors with widths set to three times the standard deviation on either side of the empirically determined parameter values, as suggested by [9] and [6], who used a similar modelling approach:

$$\begin{gathered} 0 < r_s/[kpc] < 40 \\ 0 < \rho_0/[GeVcm^{-3}] < 1 \\ 1 < M_{b,inner}/[10^7 \times M_\odot] < 7 \\ 8.6 < M_{b,outer}/[10^9 \times M_\odot] < 9.8 \\ 6 < M_{dc}/[10^{10} \times M_\odot] < 18 \end{gathered} \tag{6}$$

We used a Gaussian likelihood over the dataset's bins since the tracers are Gaussian-distributed around the reported weighted average velocity [4]. The masses of the stellar components were kept free due to their model-dependent nature, but we *can* impose additional constraints by assuming they too are independently Gaussian distributed around measurements from [6], and incorporate this into the likelihood (Eq. 7):

$$P(d|\Theta, M_{b,inner}, M_{b,outer}, M_{disk}) = \prod_{i=1}^{m} \left\{ \frac{1}{\sqrt{2\pi\sigma_{\bar{v},i}}} \exp\left[-\frac{1}{2} \frac{\left(v_c(r_i, \Theta, M_{b,inner}, M_{b,outer}, M_{disk}) - \bar{v}_i\right)^2}{\sigma^2_{\bar{v},i}} \right] \right\}$$
$$\times \frac{1}{\sqrt{2\pi\sigma_{M_{b,outer}}}} \exp\left[-\frac{1}{2} \frac{\left(M_{b,outer} - M^{\text{obs}}_{b,outer}\right)^2}{\sigma^2_{M_{b,outer}}} \right] \times \frac{1}{\sqrt{2\pi\sigma_{M_{b,inner}}}} \exp\left[-\frac{1}{2} \frac{\left(M_{b,inner} - M^{\text{obs}}_{b,inner}\right)^2}{\sigma^2_{M_{b,inner}}} \right] \tag{7}$$
$$\times \frac{1}{\sqrt{2\pi\sigma_{M_{disk}}}} \exp\left[-\frac{1}{2} \frac{\left(M_{disk} - M^{\text{obs}}_{disk}\right)^2}{\sigma^2_{M_{disk}}} \right]$$

where the index i runs over each bin in the dataset, $\Theta = (r_s, \rho_0)$, and the superscript *obs* refers to observed (i.e. previously empirically determined) values. The prior model predictive graphs of both models can be found in Appendix C.

The posterior is finally given by multiplying equations 6 and 7 and ignoring the evidence as a normalization factor.

3 Model Fitting & Comparision

The posterior was sampled using the Markov Chain Monte Carlo (MCMC) algorithm, implemented using the `emcee` Python package. The mode of the posterior (MAP values) were found using the Nelder-Mead minimizer from the `scipy` package and fed as the initial positions of the walkers. The sampler used 25000 steps and 50 walkers, resulting in ∼600 samples after removing the burn-in and thinning by half the highest autocorrelation times. The trace plots in Appendix D show good signs of mixing with no obvious drifts, trends, or biases, which confirms the sampler's efficiency.

Figure 1 and Figure 2 compare the corner plots and fits respectively, including the MAP estimates and 1σ confidence intervals. Table I provides a summary of the parameter estimates from the sampler for both the ring-less and ringed models, displaying results with and without the 10 to 20 kpc region in the former case.

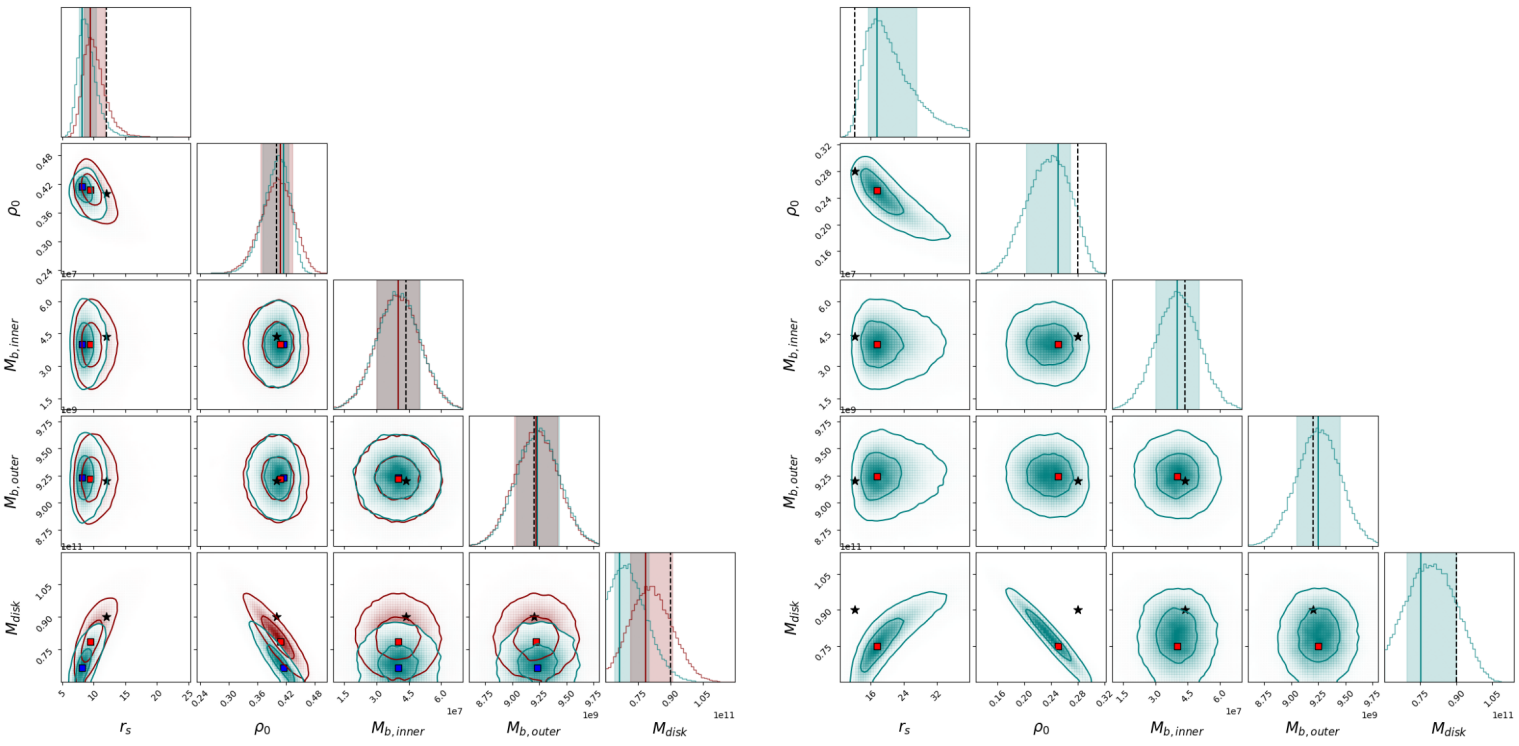

Figure 1: **Left:** Corner plot results from model 1 made up of a bulge, stellar disk and NFW dark matter profile. Blue shows results when the 10 to 20 kpc is included, and red shows when they are removed from the dataset. **Right:** Corner plot results from model 2, which included an additional contribution from the dark matter rings. The shaded region shows the 1σ confidence interval, the square markers and vertical lines show corresponding MAP values. Literature values are demarcated in black.

	$\mathbf{r_s}$ **(kpc)**	ρ_0 **(GeV cm^{-3})**	$\mathbf{M_{b,inner}}$ **(x $10^7 M\odot$)**	$\mathbf{M_{b,inner}}$ **(x $10^9 M\odot$)**	$\mathbf{M_{disk}}$ **(x $10^{10} M\odot$)**	χ^2, **PTE**	**DIC** $\mathbf{p_D}$, $\mathbf{p_v}$	**Bayes ratio**
NFW model								
With 10-20 kpc	9.04 ± 1.6	0.3979 ± 0.028	4.01 ± 1	9.2 ± 0.2	7.21 ± 0.79	55.1 0.036	-6326.6 4.9, 4.9	
Without 10-20 kpc	10.13 ± 1.8	0.400 ± 0.034	3.994 ± 0.99	9.22 ± 0.2	8.114 ± 0.96			58.06 ± 9.8
NFW + rings model	20.97 ± 6	1.170 ± 0.031	4.01 ± 0.99	9.25 ± 0.2	7.97 ± 0.97	53.1 0.053	-6332.0 4.8, 4.3	
Theoretical values	10 ± 0.5	0.40 ± 0.04 1.3 ± 0.3	4.36 ± 1	9.2 ± 0.2	9 ± 1			

Table I: Summary of results from the MCMC analysis. Parameter values are reported as the mean and standard deviation of the samples. Theoretical values are taken from [5] and [6] who used a similar component breakdown of the galaxy.

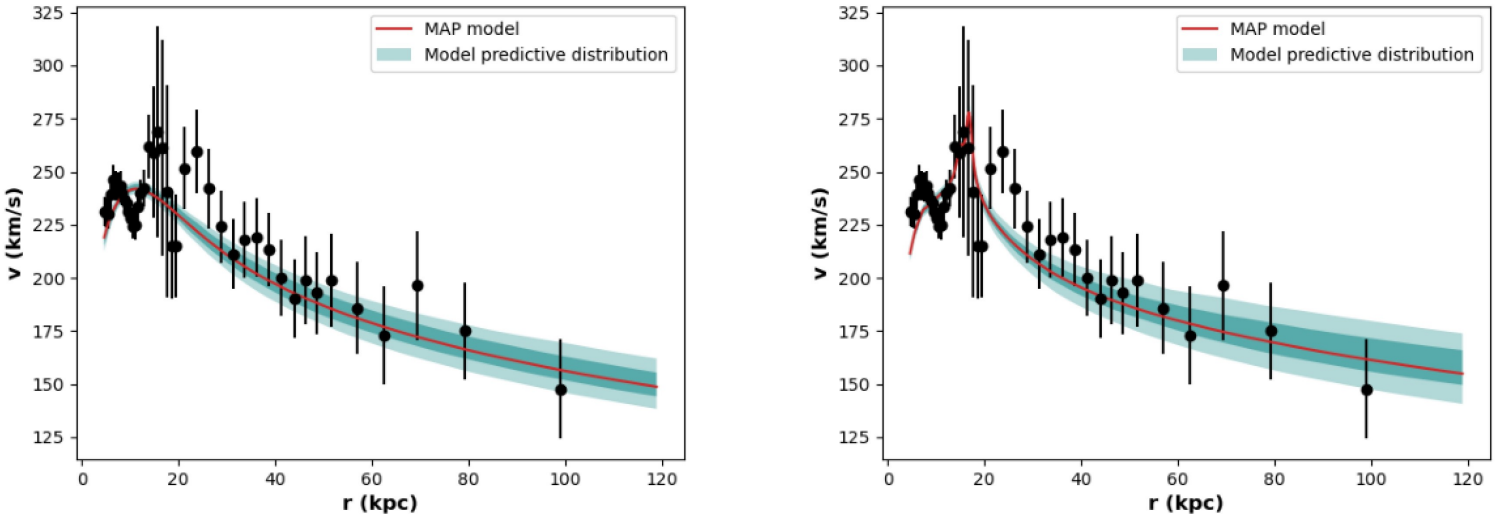

Figure 2: **Left:** Fit results for model 1, made up of a bulge, stellar disk and NFW dark matter profile. **Right:** Fit results including an additional contribution from the dark matter rings. The shaded regions indicate the 1σ and 2σ confidence intervals.

From these results, it is evident that for both models, the parameters align closely with the literature values and, in most cases, fall within the 1σ confidence interval. For the ringless model, the scale radius, dark matter density, and disk mass show differences when the 10-20kpc region is removed from the dataset. However, the standard deviations overlap for all parameters despite the wide priors that were used. The values obtained after removing data points align better with [6], especially for our parameter of interest, ρ_0. In Figure 1, we observe that while the bulge parameters are mostly independent, the stellar disk mass and the dark matter profile parameters show varying signs of correlation. This is to be expected- as mentioned in Section 2, the datapoints start at ∼5kpc- well beyond the scale of the inner and outer bulges, and thus the model is insensitive to the exact features of the bulge. At larger radii however, both the disk contribution and dark matter profile start to become comparable.

The parameter correlations become more pronounced in the ringed model, particularly between ρ_0 and r_s. This is likely because the additional contribution from the dark matter rings amplifies small changes in the parameters, making them more reactive to each other. We also observe that in general, the disk mass and, more notably, the scale radius of the dark matter profile are poorly constrained. As the disk mass increases, the contribution from the NFW profile has to decrease correspondingly. The dark matter rings then become more significant, and they potentially influence the scale radius by pushing it outwards to larger radii. The results estimate the scale radius to be nearly double the literature value in the presence of the dark matter rings, despite the disk mass remaining comparable to the first model.

The local dark matter density value of the ringed model is slightly lower than the one found by [5], but it falls within the bounds of their uncertainty. The ringed model's estimate is nearly three times higher than the first model's, whose value is robust even without the presence of the 10 to 20kpc datapoints. This is an important result for Earth-based direct detection experiments of dark matter.

We also conducted a quantitative model comparison with three metrics, the results of which are summarised in Table I. As the data is Gaussian distributed, a natural choice for a test statistic is the χ^2 value, which evaluates the goodness of fit of

the MAP values. The DIC metric combines the MAP value with the results from the sampler. Conversely, the Bayes ratio (Model 2/Model 1) is calculated independently of point estimates using the Bayesian evidence which was sampled from using the `dynasty` Python package. All three metrics suggest that the dark matter ring model is a better fit. However, while the χ^2 and DIC values indicate a slight improvement, the Bayes ratio shows a more dramatic result. As the same parameters were used in both models, the higher marginal likelihood shows that the ring model is more *globally* consistent in explaining the data and is thus more likely to produce good fits and perform better across the entire parameter space. This means that the dips at 11kpc and 19kpc are better explained as phenomenological features of the underlying dark matter distribution.

However, it is important to note that the Probability-To-Exceed (PTE) values are low for both models. As shown in Figure 2, it is evident that while the second model captures the peak in values around 20 kpc more effectively, it still shows a poor fit on the inner radial features. To improve this, we attempted to leave the parameters of the dark matter rings (e.g. positions, densities, Gaussian widths etc.) free. However, the fitting procedure quickly becomes complicated with signs of overparametrisation, and requires deeper theoretical understanding to interpret the accuracy of results, which is beyond the scope of this study. The positions, widths and density of the ring features were also empirically derived by [5] from a different dataset. Therefore, while the dark matter ring model provides more physically plausible predictions, its current assumptions and implementation may be inaccurate.

We used simple, axisymmetric models for the stellar components, but a more complex morphological model (e.g. one that includes stellar voids in the disk) may improve results. We also employed the canonical NFW model, whereas it's generalized version includes an additional parameter γ that controls the slope of the inner profile. We omitted this parameter from the fitting procedure by setting it to equal one which is equal to the cannonical case as, r_s and γ have often been found to be degenerate in previous studies [9]. However, a generalized NFW model (or other theorized dark matter models) may be a better fit the inner region of the rotation curve, which, as we can see in Fig. 2, is limited. Additionally, we did not include a gas component as it is a subdominant feature of our galaxy, but its inclusion may be important to obtain more accurate results. Additional restrictions to the parameters, e.g. from galaxy formation simulations, may also be able to better constrain the scale radius, and in turn, the stellar disk mass.

4 Conclusions

We investigated the Milky Way's dark matter distribution using a Bayesian methodology, employing the rotation curve method to infer its structure. Our data from Huang et. al [4] included line-of-sight velocities and galactocentric distances of stellar populations, extending out to $\sim$ 100kpc. Our parameter of interest was the local dark matter density, and the methodology also examined whether incorporating two ring-like dark matter overdensities would better align with the observed dips in the rotation curve. Our main findings can be summarised as follows:

- Using a double-exponential stellar bulge, infinitely thin stellar disk, and the canonical NFW dark matter model, we obtained parameter estimates whose 1σ confidence intervals, in most cases, contain estimates reported by existing studies. This suggests that these simplified models capture essential features of the system and remain consistent with more complex models whilst offering reduced computational cost.
- The dark matter distribution which incorporates two rings of overdensities provides the best fit to the observed rotation curve, supporting the hypothesised presence of ring-like dark matter structures in the $10 - 20$ kpc regions.
- The local dark matter density implied by combining the halo and dark matter ring model is $\rho_0 = 1.170 \pm 0.031\ GeV\ cm^{-3}$. This value is consistent with literature that estimates the local dark matter density using a ring model of dark matter distribution, and is approximately three times higher than estimates without them [5].
- Parameter correlations are notably stronger in the dark matter ring model compared to the purely canonical NFW model, especially between local dark matter density ρ_0 and dark matter halo scale radius r_s. This suggests that the presence of dark matter rings constrains these parameters and influences their relationship, causing them to be more strongly interdependent.

We see potential benefits in the focus of future investigations on more complex models to advance our understanding of this subject. For instance, fitting the NFW model with a radial-dependent inner slope parameter γ to the rotation curve may give rise to more constrained r_s parameters. Additionally, a more advanced MCMC fitting approach for of the dark matter ring parameters could refine the dark matter ring model. Our analysis relied on literature values, which may have constrained the goodness of fit and the accuracy of results, and further theoretical considerations would also improve results. Furthermore, repeating this methodology with different datasets would shed further light on potential systematic errors in the analysis.

References

[1] Karukes, E. V., Salucci, P., and Gentile, G. "The dark matter distribution in the spiral NGC 3198 out to 0.22 Rvir". In: *AA* 578 (2015), A13.

[2] Mariateresa Crosta et al. "On testing CDM and geometry-driven Milky Way rotation curve models with Gaia DR2". In: *Monthly Notices of the Royal Astronomical Society* 496.2 (Aug. 2020), pp. 2107–2122. arXiv: `1810.04445 [astro-ph.GA]`.

[3] Pablo F. de Salas. "Dark matter local density determination based on recent observations". In: *Journal of Physics: Conference Series* 1468.1 (Feb. 2020), p. 012020.

[4] Y. Huang et al. "The Milky Way's rotation curve out to 100 kpc and its constraint on the Galactic mass distribution". In: *Monthly Notices of the Royal Astronomical Society* 463.3 (Sept. 2016), pp. 2623–2639. eprint: `https://academic.oup.com/mnras/article-pdf/463/3/2623/8284485/stw2096.pdf`.

[5] de Boer W. and Weber M. "The dark matter density in the solar neighborhood reconsidered". In: *Journal of Cosmology and Astroparticle Physics* 2011.04 (Apr. 2011), p. 002.

[6] Yoshiaki Sofue. "Rotation and mass in the Milky Way and spiral galaxies". In: *Publications of the Astronomical Society of Japan* 69.1 (Dec. 2016).

[7] K. C. Freeman. "On the Disks of Spiral and S0 Galaxies". In: *apj* 160 (June 1970), p. 811.

[8] HongSheng Zhao. "Analytical models for galactic nuclei". In: *Mon. Not. Roy. Astron. Soc.* 278 (1996), pp. 488–496. arXiv: `astro-ph/9509122`.

[9] E.V. Karukes et al. "Bayesian reconstruction of the Milky Way dark matter distribution". In: *Journal of Cosmology and Astroparticle Physics* 2019.09 (Sept. 2019), 046–046.

A Link to code

The code and plots can be found **here**. If the link doesn't work, please copy and paste the following link to the Github repository:

https://github.com/captainkee25/Bayesian-MW-DM-reconstruction-main.git

B The Data

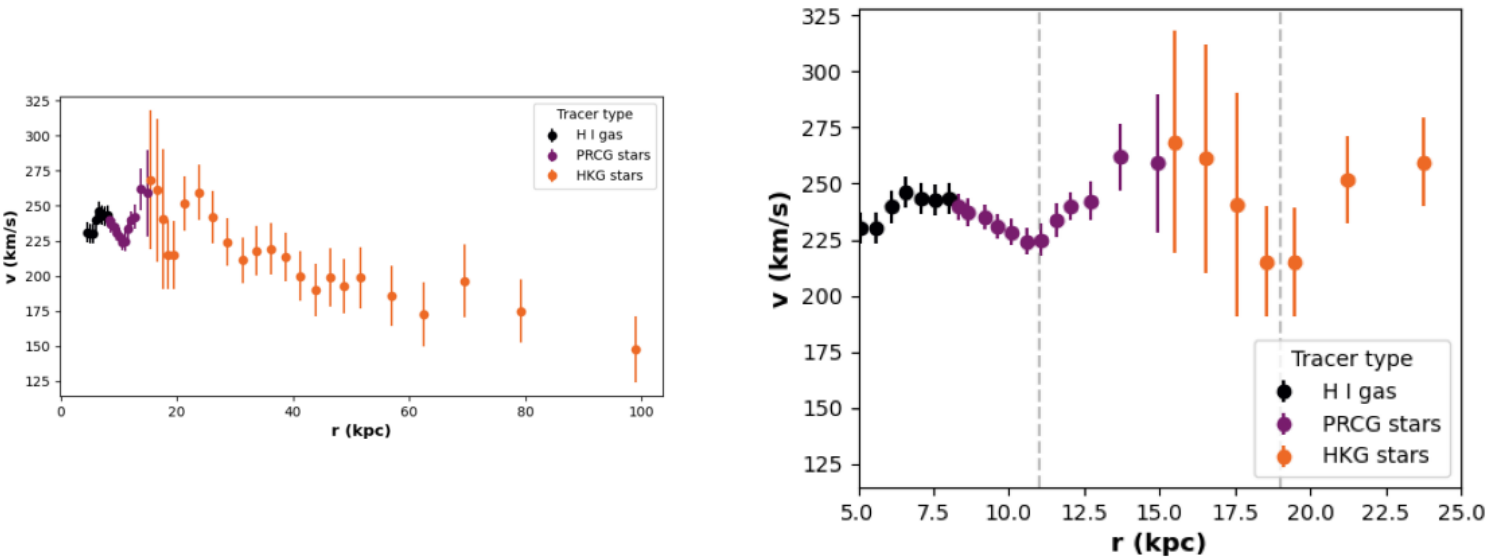

Figure 3: **Left:** Full rotation curve of the Milky Way as reported by [4], colour coded to indiciate which tracers were used for each datapoint. **Right:** Same rotation curve zoomed-in to the 10 to 20 kpc region to highlight the dips at 11kpc and 19kpc (grey dashed lines)

.

C Prior model predictive

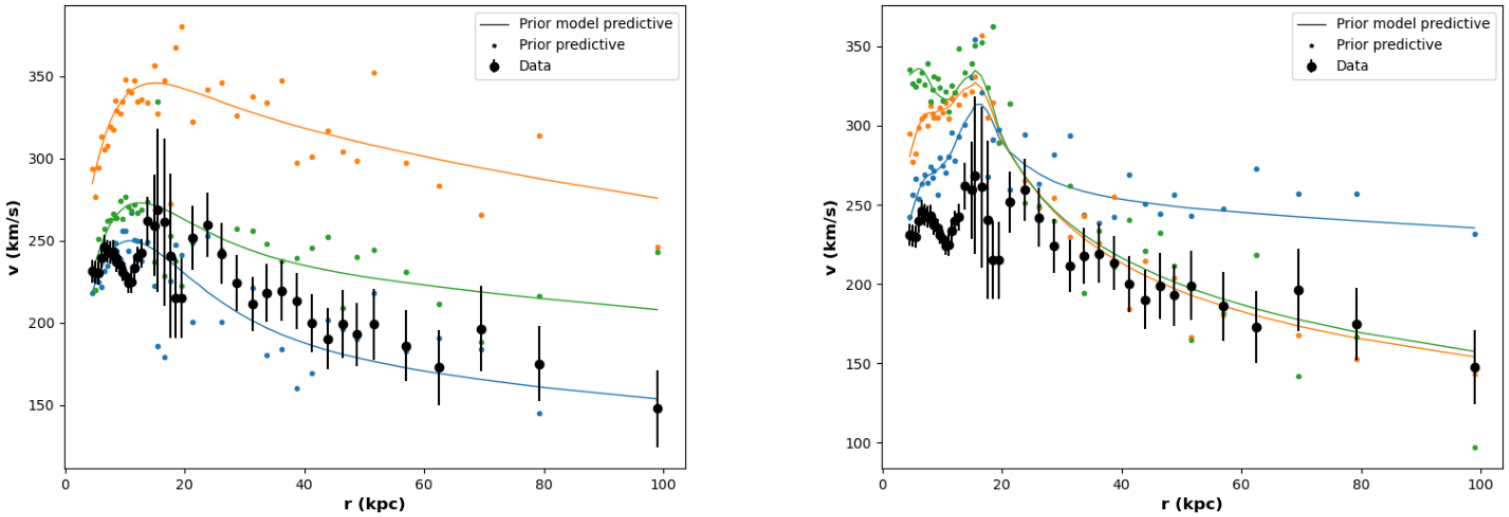

Figure 4: **Left:** Prior predictive with Gaussian noise added for a random selection of samples from the posterior for model 1 composed of a bulge, disk and NFW dark matter profile. **Right:** Prior predictive with Gaussian noise added for a random selection of samples from the posterior for model 2, which includes an additional contribution from dark matter rings.

D Trace plots

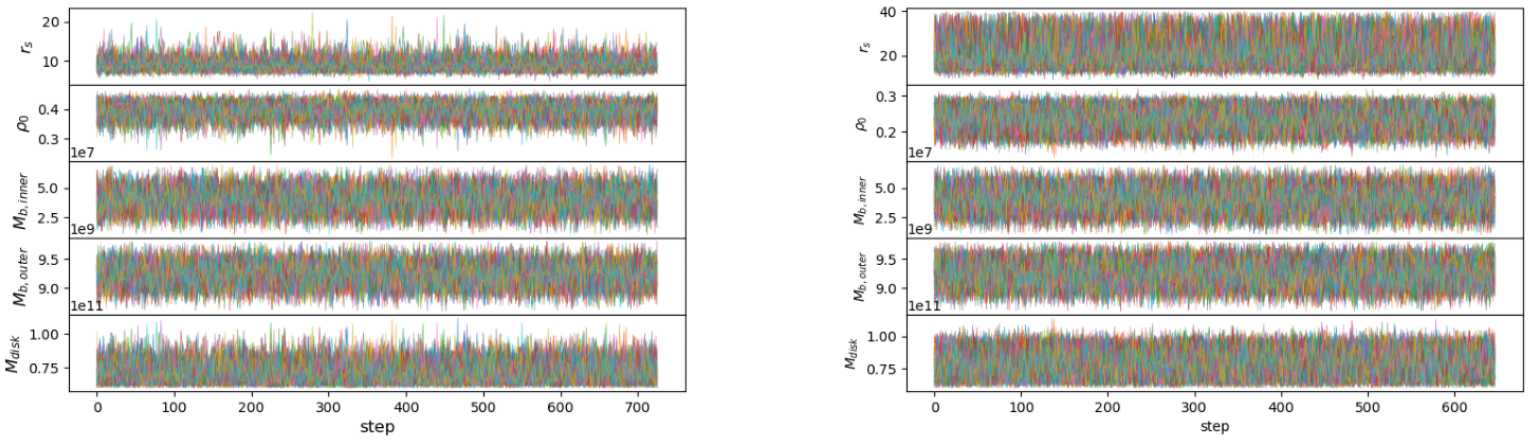

Figure 5: **Left:** Thinned trace plots with burn-in removed for model 1 **Right:** Thinned trace plots with burn-in removed for model 2.